RESEARCH ARTICLE

Kinetics and isotherm studies for the adsorption of Cu(II) from aqueous solution by carbon-based matrix formed using para-nitroacetanilide

T. M. M. K. Bandara* and V. N. Seneviratne

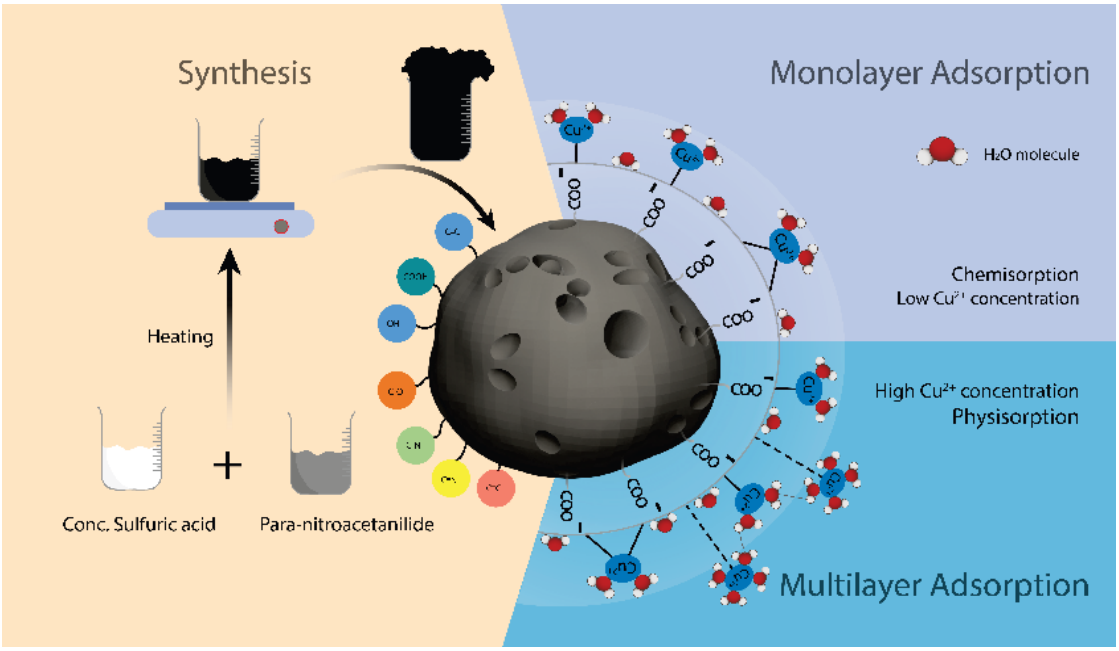

Highlights

- A new adsorbent was prepared upon heating para-nitroacetanilide and concentrated sulfuric acid.
- The adsorption behavior of Cu^{2+} on the adsorbent was studied.
- Maximum Cu^{2+} removal (68%) was obtained at pH 6, with 0.125 g of adsorbent, 50 min shaking time, and 96.25 mg L^{-1} initial concentration of Cu^{2+} solution.
- Adsorption data fit the Freundlich isotherm, and adsorption kinetics agreed pseudo-second-order kinetics.
- Due to the high removal percentage, it can be used in the removal of Cu^{2+} from industrial water.

Ceylon Journal of Science 51 (Special Issue) 2022: 521-529
DOI: http://doi.org/10.4038/cjs.v51i5.8079

RESEARCH ARTICLE

Kinetics and isotherm studies for the adsorption of Cu(II) from aqueous solution by carbon-based matrix formed using para-nitroacetanilide

T. M. M. K. Bandara* and V. N. Seneviratne

Department of Chemistry, Faculty of Science, University of Peradeniya, Peradeniya, 20400, Sri Lanka

Received: 30/06/2021; Accepted:30/03/2022

Abstract: Pollution of water is a pragmatic problem in the world today. Contamination by heavy metals and dyes is a major concern of water pollution. This study examines a new adsorbent made by the reaction between para-nitroacetanilide and concentrated sulfuric acid and is the first-ever study carried out to the best of our knowledge. The adsorption of Cu^{2+} has been studied on this adsorbent as a preliminary study. The prepared material was characterized using Fourier Transform Infrared Spectroscopy (FTIR), Scanning Electron Microscopy (SEM), X-ray Fluorescence Spectroscopy (XRF), Powder X-ray Diffraction (PXRD) and point of zero charges (pzc) analysis. The average pore diameter obtained from SEM analysis was 2 µm, concluding that the adsorbent has a desirable morphology for better adsorption. The adsorption experiments were carried out as a function of pH, shaking time, initial Cu^{2+} concentration, and adsorbent dosage. The adsorption kinetics at low concentrations (34.50 mg L^{-1} = 1.5×10^{-7} mol m^{-3}) follows pseudo-second-order kinetics with an R^2 value of 0.99, suggesting a chemisorption process. The adsorption data agree with the Freundlich isotherm at higher concentrations (varying from 17.21 mg L^{-1} (7×10^{-8} mol m^{-3}) to 96.25 mg L^{-1} (3.6×10^{-7} mol m^{-3}) revealing multilayer adsorption, amounting to a maximum adsorption capacity of 8.31 mg g^{-1} at 25 °C.

***Keywords*:** Para-nitroacetanilide; copper adsorption; heavy metal removal; chemisorption; physisorption.

INTRODUCTION

Water pollution has become a severe problem in the world today. Water is generally referred to as polluted when its physical, chemical or biological parameters become harmful to man or aquatic life (Ömer *et al*., 2016). Pollution changes the physical characteristics of water such as colour, odour, temperature, turbidity, density, etc., and chemical aspects such as acidity, alkalinity, pH, the content of dissolved solids, suspended solids, dissolved oxygen, heavy metal ions, anions, pesticides, and other organic pollutants as well. Biological water pollution may occur due to the presence of harmful disease-causing bacteria, algal blooms, and the decomposition of animal and plant matter. In addition to all these processes, anthropological activities also introduce various heavy metals into waterways. Among the myriad pollutants encountered, heavy metals are known to be the most hazardous substances in contaminated water. Compared to other heavy metals, the usage of copper has increased, even though it belongs to the group of seriously hazardous heavy metals. Industries such as electroplating, leather tanning, paint, textile, steel, mining, metal processing, and battery manufacturing extensively release copper to natural water bodies (Rais *et al*., 2011). With regard to the discharge of copper into water bodies as industrial effluents, the permissible limit is 1.5 mg L^{-1} (Amarasiri, 2015). Nonetheless, copper is an essential nutrient to higher plants and animal life, where it acts as a cofactor of enzymes and as an antimicrobial agent (Shakila *et al*., 2020). Copper and copper-containing compounds, such as copper sulfate, copper oxides, copper chloride, and copper carbonate are used in commercial industries. But copper shows adverse effects on many components of the ecosystem, primarily due to its ability to travel long distances in the atmosphere before they are deposited. As copper metals are non-degradable, they can be found in air, soil, and water. Since plants absorb nutrients and water from the soil, copper in the environment can easily enter plant bodies. Copper present in water bodies also enters living organisms. Consumption of such organisms leads to bioaccumulation and biomagnification of copper in higher members of the food chain. Exposure to copper has a likelihood of resulting in harmful effects such as liver and kidney damage, mental health problems, and brain and heart failure (Rais *et al*., 2011). To reduce water pollution caused by copper, various methods have been employed. These include chemical precipitation, evaporation, electrochemical treatment, and the use of ion-exchange resins on contaminated effluents. These methods are expensive and sometimes ineffective, especially when copper is present in very low concentrations. Several techniques, including adsorption, electrochemical precipitation, and reverse osmosis, are still used for the treatment of effluents containing copper metal ions (Volzone and Garrido, 2008). Out of all these methods, adsorption is the most versatile and widely used method owing to its ease of use. Much research has been carried out to study the removal of copper metal using a variety of adsorbents (Dongxiao *et al*., 2019). Activated carbon, albeit expensive, is the most commonly used adsorbent because of its high level of effectiveness (Yu *et al*., 2001; Chand *et al*., 2009). This has attracted the investigation of novel, cost-effective materials for adsorption. This study focuses on a new adsorbent formed by the reaction between Para–

**Corresponding Author's Email: tm.madushani1111@gmail.com*
https://orcid.org/0000-0001-7387-8250

nitro acetanilide and concentrated sulfuric acid forming a highly porous substrate, in the presence of heat. Para-nitroacetanilide is a readily available and relatively cheap material, and it gives a high percentage yield of carbon (96%). As of this moment of publication, we are not aware of the exact chemical transformation - but dehydration and redox reactions are thought to take place. The reaction produces amorphous elemental carbon and various surface functional groups such as –COOH and –OH are incorporated onto the surface. Gases such as SO_2, N_2, CO_2, and H_2O are evolved in the reaction. Trapping these gases on the solid matrix, a porous structure would form. These properties will make this material a potential candidate for the adsorption of metal ions. The work described here demonstrates how this highly porous adsorbent has been used to remove Cu^{2+} ions from an aqueous solution. The adsorption behavior of the produced material was studied as a function of pH, shaking time, initial Cu^{2+} concentration, and adsorbent dosage. The isotherm studies and adsorption kinetics were also studied subsequently.

MATERIALS AND METHODS

Materials

Para-nitroacetanilide (purity- 98%), copper(II) sulfatepentahydrate (purity-99.9%), and all other chemicals were purchased from Sigma Aldrich, UK, and were used as they were received. All the experiments were conducted under static conditions, with adsorbent particles of size <120 µm.

Preparation of the adsorbent

Para-nitroacetanilide (5.012 g) and concentrated sulfuric acid (5 mL) were added to a small beaker. This mixture was made homogeneous by stirring. It was heated to 350 - 450 ℃. A black foam-like solid product was formed. It was washed with copious amounts of distilled water until a pH of 7 was obtained, grounded, and sieved using a 120 µm sieve.

Characterization

Standard pellets were prepared by mixing (30:1 ratio) fused KBr with each powdered adsorbent, before and after the treatment with Cu^{2+} for Fourier Transform Infrared spectroscopic analysis using Shimandu Prestige-21, in the scan range of 4000-400 cm^{-1}. XRF analysis was carried out using the adsorbent, before and after the adsorption of Cu^{2+}. The Cu^{2+} adsorbed adsorbent was obtained by stirring the adsorbent in a solution of Cu^{2+} and then filtering the suspension. The samples of Cu^{2+} adsorbed matrices obtained were washed with distilled water several times, air-dried, and used for XRF analysis with a Fischerscope Model-DF500FG-456 spectrometers. SEM images of the adsorbent, before and after the treatment of Cu^{2+} were taken using a Scanning Electron Microscope (Model-ZEISS EVOLS15). After the adsorption of Cu^{2+}, adsorbent particles were filtered, washed, dried, and then used for SEM analysis. They were used to investigate the surface morphology of the composite. Adsorbent synthesized was characterized further by taking PXRD patterns using Siemens D 5000 Powder X-ray diffractometer equipped with Cu Kα radiation in the scanning angle (2θ) ranging from 3° to 45° at the scanning rate of 1°/ second.

Zero-point charge analysis

The pH at the point of zero charges was measured by using the pH drift method (Kousmulski, 2006). The pH of a solution of 0.0001 mol m^{-3} $NaNO_3$ solution was adjusted to be between 2 and 12 by adding either NaOH or HCl. A 0.150 g of adsorbent was added to 50.00 mL of $NaNO_3$ solution. After 24 h the final pH was recorded. The graph of final pH vs initial pH was used to determine the zero-point charge. The point considered as pH_{zpc} is calculated at the point at which the initial and final pH values were equal.

Optimization of experimental parameters

Weighed masses of adsorbent were added to 50.00 mL of Cu^{2+} solutions placed in small jars and pH values were measured. Each sample was shaken at a speed of 150 rpm for a specified period and was allowed to settle for 3 h. Next, the supernatant was pipetted out. Finally, the supernatant concentration was measured using Spectro-Electronic M Series Atomic Absorption Spectrophotometer (AAS) from Agilent technologies. The percentage removal was calculated using the following equation,

$$\textbf{percentage removal} = \frac{C_i - C_f}{C_i} \times 100\%$$

where, C_i and C_f (ppm or mol m^{-3}) are the initial and final concentrations of the Cu^{2+} in solution.

The concentrations C_i and C_f were determined with the use of a calibration curve constructed daily using a standard solution of Cu^{2+} to improve the precision of measurements. All the experiments were carried out in triplicate, and average values were reported.

Many trials were carried out with solutions of low concentration Cu^{2+}, but the absorbance values were negative. Hence, to optimize the parameters, a high concentration of Cu^{2+} was used.

Optimization of solution pH

The effect of the initial solution pH on the removal of Cu^{2+} was studied at different pH values ranging from 2 to 10 using a 38.50 mg L^{-1} (1.5×10^{-7} mol m^{-3}) Cu^{2+} solution. Solutions of different pH values were prepared using HNO_3 and NaOH. An experiment for the optimization of initial solution pH was conducted using 0.125 g of adsorbent and 50 min shaking time.

Optimization of adsorbent dosage

Different masses of adsorbent were weighed accurately ranging from 0.025 g to 0.250 g. Then 50.00 cm^3 samples of Cu^{2+} with a concentration of 32.50 mg L^{-1} (1.3×10^{-7} mol m^{-3}) solutions were added to weighed adsorbent samples placed in separate jars. Then the samples were stirred thoroughly at a speed of 150 rpm for 20 min followed by 3 h of settling time. The pH of the initial Cu^{2+} solution was maintained at a value of 6.0 throughout the experiment.

Optimization of shaking time

Cu^{2+} solution (50.00 cm^3, 36.25 mg L^{-1} (1.5×10^{-7} mol m^{-3}),

pH = 6.0) was separately stirred at a speed of 150 rpm with an optimized dosage of adsorbent for different shaking times ranging from 10 min to 70 min followed by 3 h of settling time.

Optimization of initial Cu^{2+} concentration

Adsorbent (0.125 g) was added to 50.00 cm^3 of Cu^{2+} solution (ranging from 17.21 mg L^{-1} (7×10^{-8} mol m^{-3}) – 127.23 ppm (5.1×10^{-7} mol m^{-3})), placed in small jars and the pH was adjusted to 6. Each sample was shaken at a speed of 150 rpm for 50 min of shaking time and was allowed to settle for 3 h.

Isotherm studies

First, many trials were carried out to find the best range of Cu^{2+} ion concentration. Then Cu^{2+} ion solution of initial concentration varying from 17.21 mg L^{-1} (7×10^{-8} mol m^{-3}) to 96.25 mg L^{-1} mg L^{-1} (3.7×10^{-7} mol m^{-3}) was shaken with the adsorbent under optimized conditions of shaking time and pH. Each solution was then allowed to reach equilibrium, and the concentration of Cu^{2+} ions in the supernatant solution was measured. Measurements were carried out in triplicates. The extent of adsorption was calculated as the mass of copper adsorbed (in mg) on 0.125 g of adsorbent (mg g^{-1}). A graph of the extent of adsorption versus initial Cu^{2+} ion concentration was plotted. Adsorption data were also analyzed to check the validity of the Langmuir and Freundlich isotherms, and the isotherm constants of these models were calculated.

Kinetics studies

Kinetic experiments were carried out at ambient temperature (25 ℃) to understand the interactions of Cu^{2+} with the adsorbent. 0.625 g of adsorbent was treated with 980 cm^3 of 34.50 mg L^{-1} (1.4×10^{-7} mol m^{-3}) Cu^{2+} solution and was allowed to stir slowly with a magnetic stirrer. While the solution was being stirred, 5.00 cm^3 samples of the supernatant solution were withdrawn at 5 min intervals for the next 150 min. Then the solution was filtered and the concentration of Cu^{2+} in the samples withdrawn was determined by AAS, and percentage adsorption was calculated. The order of the reaction, such as pseudo-first-order and the second order was calculated by applying kinetic models on this data.

RESULTS

Characterization

FTIR analysis

The new adsorbent consists of different functional groups that can be identified using FTIR. Further, if any metal-oxygen bonds are formed, they can also be identified using FTIR data. Generally, the adsorption capacities of an adsorbent depend on the chemical affinities of these functional groups and the porosity of the adsorbent (Etim *et al*., 2000). Figure 1 shows the FTIR spectra before and after adsorption.

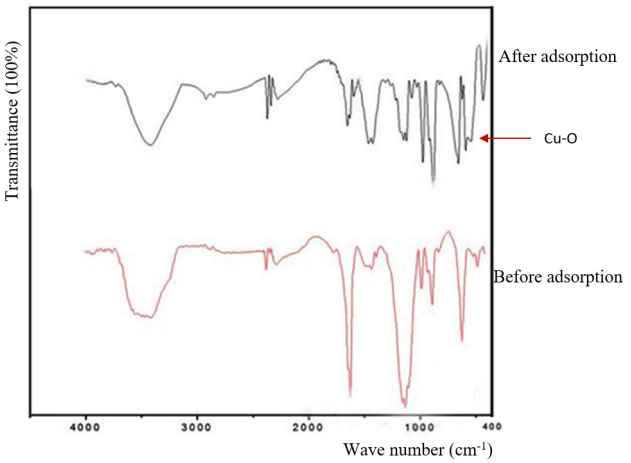

Figure 1: FTIR spectrum of adsorbent before and after adsorption of Cu^{2+}.

Before Adsorption - the FTIR spectrum showed bands at 3504 cm^{-1} and 1433 cm^{-1}due to stretching and bending vibration of O-H respectively. The band at 2366 cm^{-1} is due to either C≡N or C≡C. The band at 1627 cm^{-1} is due to either C=C or a -NO_2 group or α,β-unsaturated C=O. The band at 1130 cm^{-1} is due to a either C-O or C-N group.

After Adsorption - the spectrum showed bands at 3433 cm^{-1} and 1457 cm^{-1} due to O-H stretching and O-H bending. The band at 2370 cm^{-1} is due to either C≡N or C≡C. The band at 1648 cm^{-1} is due to either C=C or a -NO_2 group or α,β-unsaturated carbonyl group. The band at 1144 cm^{-1} is due to either a C-N or C-C group. The additional band at 650 cm^{-1} is due to the Cu-O bond (Benjamin and Leckie, 1981).

Broadband for O-H stretch, a sharp band for C=O, C-O stretch, and O-H bend bands revealed the presence of a COOH group. The FTIR spectrum after adsorption indicates the adsorption of Cu^{2+} on to adsorbent by chemical forces instead of physical forces. This is indicated by the increment or decrement of the band positions of O-H stretching, O-H bending, C=C or -NO_2 group or α,β-unsaturated C=O, and C-O or C-N groups. There also has been the presence of an additional band at 650 cm^{-1} that is due to the Cu-O bond. That concludes Cu^{2+} ions have bound to the adsorbent via the deprotonated COOH group.

XRF analysis

XRF analysis provides information on the metal present in the sample (Figure 2a). There are no peaks related to heavy metals in the original sample. Comparison between XRF spectra clearly indicates Cu^{2+} adsorbed onto the adsorbent. Even after several piles of washing of the material with distilled water, the peak appeared.

PXRD analysis

PXRD data clearly shows a broad peak centering the 2θ value ~25.5° proving that the adsorbent formed in the synthesis is elemental carbon in the amorphous form (Figure 2b)(Manoj, Kunjomana, 2012).

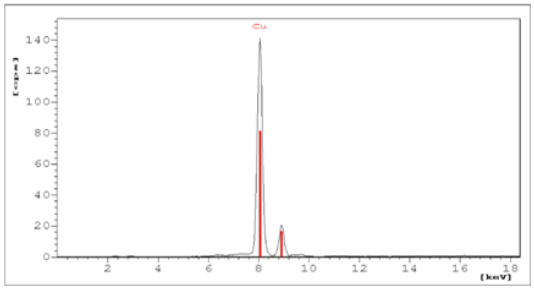

(a)

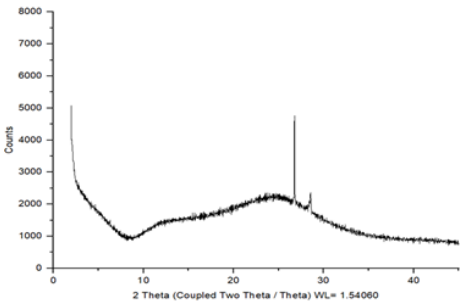

(b)

Figure 2: (a) XRF spectrum of adsorbent after adsorption of Cu^{2+} (b) PXRD pattern of the adsorbent

SEM analysis

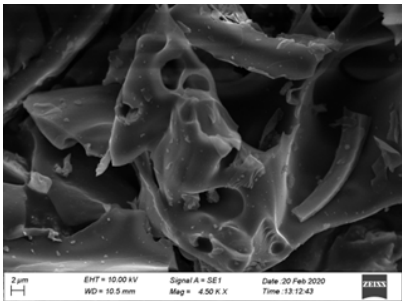

Before adsorption

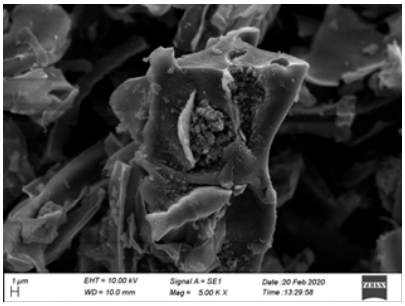

After adsorption

Figure 03: SEM images of adsorbent before and after adsorption of Cu^{2+}.

SEM images before adsorption indicate a porous surface with an average pore size of 2 µm and a rough structure which is one of the key factors for increased adsorption capacity (Figure 3). SEM images after adsorption show much smoother surface morphology. It is evident that upon adsorbing Cu^{2+} ions, the surface structure of the adsorbent has changed.

Zero-point charge determination

It is necessary to determine the point of zero charges of the adsorbent to understand the adsorption mechanism. The point of zero charge is described as the pH at which the net charge of the total particle surface is equal to zero (Kousmulski, 2006). The zero-point charge is the point at which the initial and final pH value is equal. At that point, the adsorbent charge is neutral. Below this value, the surface is positively charged, whereas above this value the surface is negatively charged. It is easier to adsorb a cation onto a negatively charged surface and anion onto a positively charged species as the surface functional groups electrostatically interact with the species (Kousmulski, 2006).

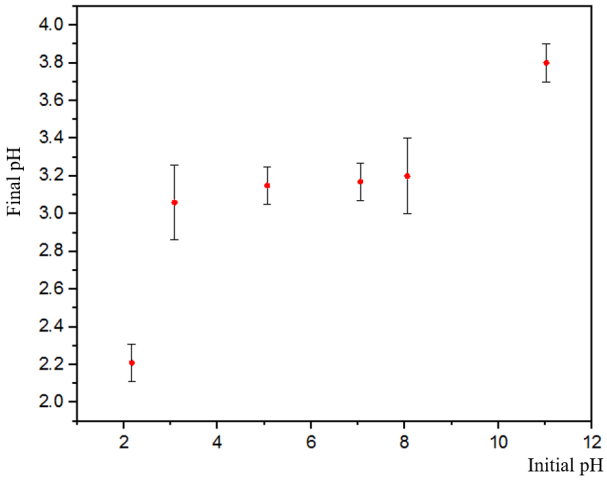

Figure 4: Graph of final pH vs initial pH.
(24 h shaking time, 0.150 g of adsorbent, 0.0001 mol m^{-3} $NaNO_3$ 50 mL solution).

With the analysis of data obtained from Figure 4, the pH at the (pH_{zpc}) was found to be 3.

Optimizing conditions for adsorption

Optimization of pH

The pH of effluents is an important parameter that affects the removal of heavy metal ions. Furthermore, the solubility of a compound and the removal percentage of Cu^{2+}depend on the pH of the solution. Thus, adjustment of the pH of the solution is vital in removing Cu^{2+} ions. Figure 5 shows the percentage removal of Cu^{2+} at different pH values.

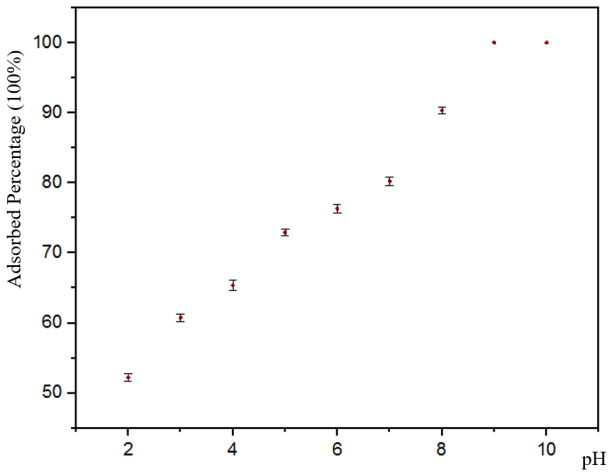

Figure 5: Percentage removal of Cu^{2+} at different pH.
(50 min shaking time, 3 h settling time, 0.125 g of adsorbent, 38.50 mg L^{-1} (1.5×10^{-7} mol m^{-3}) of Cu^{2+} 50 mL solution).

It is now established that the surface of the adsorbent is negatively charged above pH 3. The negatively charged adsorbent which contains anionic surface groups will interact with Cu^{2+} cations by electrostatic attractions for high adsorption of Cu^{2+}.The optimum pH for the adsorption was concluded as pH 6 considering the solubility product of copper hydroxide and surface charge of the adsorbent. At pH 6, the surface of the adsorbent is negatively charged due to the deprotonation of some carboxylic groups in the adsorbent. These negative charges make favorable electrostatic interactions with positively charged Cu^{2+} ions resulting in higher percentage removal. At any other pH below 3, the surface charge is positive and will make repulsive forces between the positively charged adsorbent and Cu^{2+} ions. This leads to lower adsorption. The percentage removal between pH 3-5, has increased as the surface charge is negative. Above pH 6, there is only a low amount of Cu^{2+} ions available in the solution as most of it will precipitate as copper hydroxide ($K_{sp} = 1.9 \times 10^{-19}$ mol^3 L^{-3}) (Yu *et al*., 2001; Jonathan *et al*., 2006; Banerjee and Chattopadhyaya, 2017). There is a gradual increase of the adsorbed percentage of Cu^{2+}within the pH range 3-6 due to the gradual deprotonation of COOH groups.

Optimization of shaken time

Figure 6 shows how the amount adsorbed varies with shaking time.

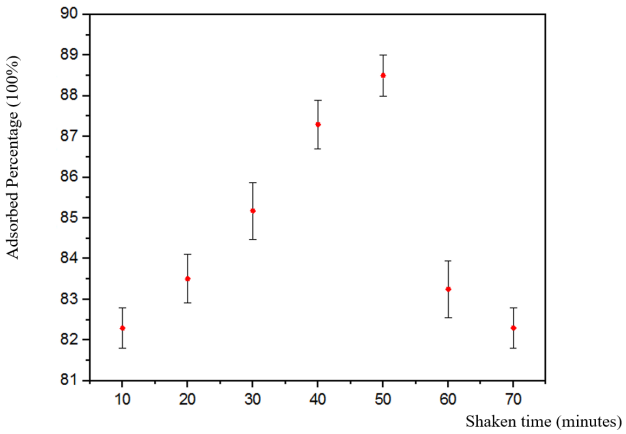

Figure 6: Percentage removal of Cu^{2+} at different shaken times.

(pH:6, 3 h settling time, 0.125 g of adsorbent, 36.25 mg L^{-1} (1.5×10^{-7} mol m^{-3}) of Cu^{2+} 50 mL solution).

The extent of removal of metal ions under investigation increases considerably during the initial 50 min and decreases thereafter. More adsorption sites are available on the surface for Cu^{2+} adsorption at the beginning. Therefore, the adsorbed percentage increases during the initial 50 min. After 50 min, the low percentage of Cu^{2+} ions adsorbed to the adsorbent implies that some desorption takes place as a consequence of stirring.

Optimization of adsorbent dosage

Figure 7 illustrates the percentage removal of Cu^{2+} at different adsorbent dosages.

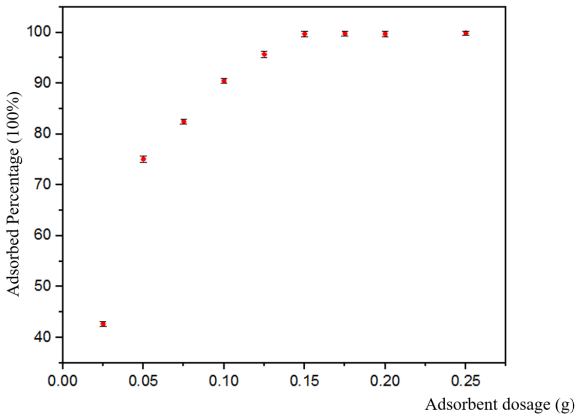

Figure 7: Percentage removal of Cu^{2+} at different adsorbent dosages.

(50 min shaking time, 3 h settling time, pH: 6, 32.50 ppm (1.3×10^{-7} mol m^{-3}) of Cu^{2+} 50 mL solution).

When the adsorbent dosage is increased, the percentage of Cu^{2+} removal will increase because of the increased number of adsorption sites. A low Cu^{2+} removal percentage was observed at a dosage of 0.025 g. It could be attributed to the presence of a lower number of adsorption sites in the composite to adsorb Cu^{2+} ions. The optimum dosage was 0.125 g. As the dosage is increased, the Cu^{2+} removal percentage becomes constant. It is because the initial number of moles of Cu^{2+} is constant, even though the numbers of adsorption sites are increased (Nandi *et al*., 2008).

Optimization of initial Cu^{2+}concentration

Figure 8 shows the removal of Cu^{2+} at different initial Cu^{2+} concentrations.

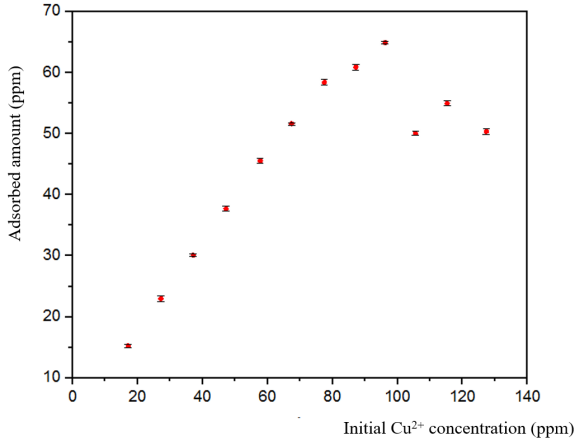

Figure 8: Removal amount of Cu^{2+}at different initial Cu^{2+} concentrations.

(50 min shaking time, 3 h settling time, 0.125 g of adsorbent, pH: 6).

In optimizing the initial Cu^{2+} concentration, the adsorbent dosage was kept constant throughout the experiment while increasing the initial Cu^{2+} concentration. Therefore, a limited number of adsorption sites are available for adsorption although the concentration of adsorbate increases. Furthermore, after all these sites are occupied, the adsorbent surface is almost covered with a layer of Cu^{2+}. This situation is called a monolayer formation. After the formation of a monolayer, another layer could form on

top of the monolayer due to the secondary attractions. The optimum initial Cu^{2+} concentration was concluded to be 96.25 mg L^{-1} (3.7×10^{-7} mol m^{-3}).

Isotherm studies

Adsorption isotherms are functions that correlate the amount of adsorbate on the adsorbent with changes in concentration at a constant temperature. There is an equilibrium established between the amount of adsorbate adsorbed and the amount of adsorbent in the solution. This equilibrium relationship is described by adsorption isotherms. The Langmuir and Freundlich isotherms, which are perhaps the most popular isotherm models available, were used in this research to study Cu^{2+} behavior with the adsorbent (Mane *et al*., 2007; Pehlivan *et al*., 2008).

Langmuir isotherm model

The Langmuir equation is valid for monolayer adsorption onto a completely homogenous surface with a finite number of identical sites. Interactions are negligible between adsorbed molecules. The equation is as follows,

$$\frac{C_e}{q_e} = \frac{1}{q_{max}K_L} + \frac{C_e}{q_{max}}$$

Where, C_e, q_e, q_{max} and K_L are equilibrium concentration (mg L^{-1}), amount of adsorbed material at equilibrium (mg/g), capacity parameter (mg/g) and affinity parameter of Langmuir constant (L/mg) respectively.

Freundlich isotherm model

This is applied for non-ideal adsorption on heterogeneous surfaces and multilayer formation. The equation is as follows,

$$\ln(q_e) = \ln(K_f) + \frac{1}{n}\ln(C_e)$$

Where, q_e, K_f, n, C_e are amount of adsorbed material at equilibrium (mg/g), Freundlich isotherm constant (mg/g), dimensionless constant and equilibrium concentration (mg L^{-1}) respectively.

Figures 9 and 10 depict how these data fit Langmuir and Freundlich isotherm respectively.

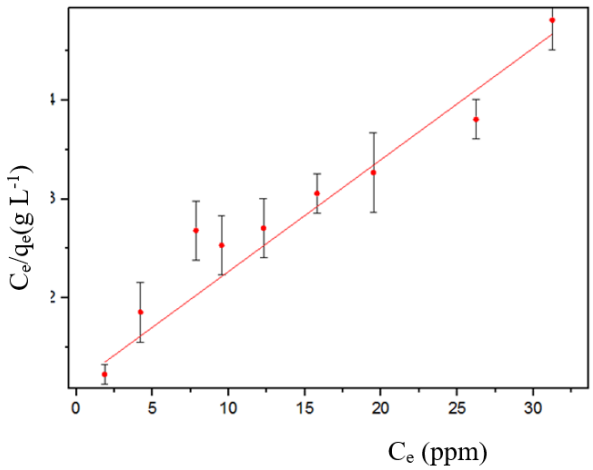

Figure 9: Behavior according to Langmuir model (25 °C).

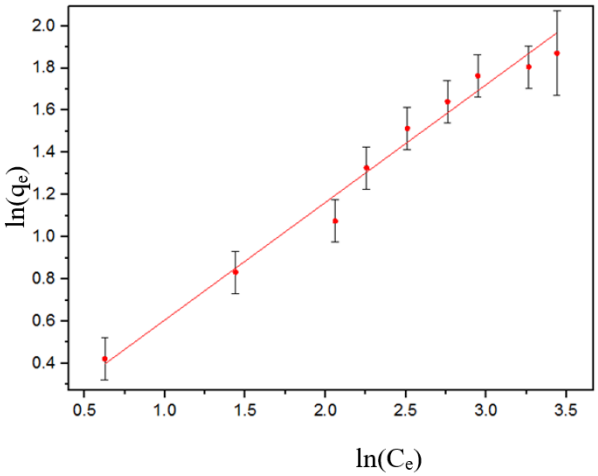

Figure 10: Behavior according to Freundlich model (25 °C).

Table 1: Data obtained Freundlich isotherm model.

Temperature (˚C)	Langmuir model		Freundlich model	
	q_{max} (mg/g)	R^2	n	R^2
25	8.31	0.94	1.88	0.98

Among the two models, the best-suited model was investigated by the magnitude of linear regression (R^2) of each model. When the R^2 value is closer to 1, it is considered the best-suited model. Since the regression value of the Freundlich isotherm is 0.98, the adsorption data fit the Freundlich isotherm at higher concentration revealing multi-layer adsorption (Wan Ngah *et al*., 2004).

Kinetics studies

Kinetic studies and equilibrium studies play an important role in understanding adsorption systems. An adsorption process involving a liquid phase and a solid phase would have multi-step reactions. This can be elaborated using kinetic studies. Kinetic studies related to the adsorption process are investigated using a constant amount of adsorbent. Keeping the concentration of one reactant constant, yields pseudo-order kinetics. Such systems are described using pseudo-order models which describe how the rate depends on the equilibrium adsorption capacity, but not on the concentration of the adsorbate. Therefore, pseudo-first-order and pseudo-second-order equations were tested (Mane *et al*., 2007; Simonin, 2016). The earliest model of kinetics based on adsorption capacity was introduced by Lagergren. It can be shown as,

$$\frac{dq_t}{dt} = k'(q_e - q_t)^n$$

Where, q_t, K', q_e, n and t are amount of adsorbate adsorbed per unit mass of adsorbent at given time, rate constant, amount of adsorbate adsorbed per unit mass of adsorbent at equilibrium , order of the reaction with respect to adsorbate and time respectively.

n=1 describes pseudo-first-order kinetics, *n*=2 -pseudo-second-order kinetics is represented.

Pseudo-first-order kinetic model

This model is based on the change of adsorbate uptake with time and indicates that the reaction is more inclined towards physisorption.

$$\ln(q_e - q_t) = \ln(q_e) - K_1 t$$

Where, K_1, q_e , q_t and t are rate constant (mg $g^{-1}min^{-1}$), amount of adsorbate adsorbed per unit mass of adsorbent at equilibrium (mg/g) amount of adsorbate adsorbed per unit mass of adsorbent at given time (mg/g) and time(min) respectively.

Pseudo-second-order kinetic model

The pseudo-second-order kinetic model is based on the assumption that the rate-limiting step is chemisorption. In this model, the adsorption rate is dependent on adsorption capacity, and not on the concentration of the adsorbate.

$$\frac{t}{q_t} = \frac{1}{K_2 q_e^2} + \frac{t}{q_e}$$

Where, K_2 , q_e , q_t and t are rate constant (g mg^{-1} min^{-1}), amount of adsorbate adsorbed per unit mass of adsorbent at equilibrium (mg/g), amount of adsorbate adsorbed per unit mass of adsorbent at given time (mg/g) and time(min) respectively.

The following figures 11 and 12 represent how data obtained match pseudo-first-order and pseudo-second-order kinetics.

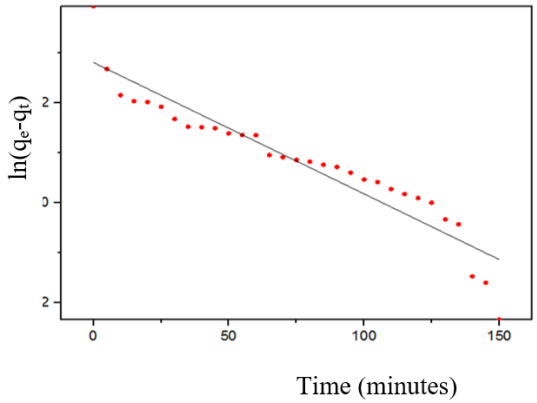

Figure 11: Pseudo first order kinetics of Cu^{2+}adsorption.

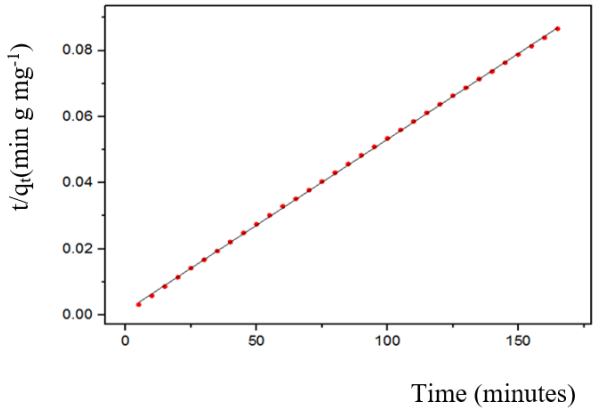

Figure 12: Pseudo second order kinetics of Cu^{2+}adsorption.

Table 2: Data obtained from kinetic models.

Pseudo first order kinetics		Pseudo second order kinetics	
K_1 (mg $g^{-1}min^{-1}$)	R^2	K_2 (g $mg^{-1}min^{-1}$)	R^2
0.026	0.86	0.035	0.99

An impressive R^2 value of 0.999 was observed for the pseudo-second-order model. Hence, this describes the adsorption process best. The assumption based on pseudo-second-order is that the rate-limiting step may be a chemisorption process. It was concluded that at low concentrations, chemisorption will take place, while multilayer adsorption takes place at a higher concentration. At low concentrations, the surrounding water molecules which are chelated with Cu^{2+} ions form hydrogen bonds with the surface. However, at higher concentrations, it tends to form multilayers because of other copper ions forming weak Van der Waals interactions with the already adsorbed Cu^{2+}-water complex.

CONCLUSION

This study investigated the adsorption of Cu^{2+} onto a new adsorbent successfully prepared by the reaction between para-nitroacetanilide and concentrated sulfuric acid as a function of pH, adsorbent dosage, shaking time, and initial Cu^{2+} concentration. The highest Cu^{2+} removal efficiency amounting to 68% was achieved through optimization of experimental parameters. The adsorption of Cu^{2+} on the substrate as a monolayer will take place at low concentrations (34.50 mg L^{-1} = 1.4×10^{-7} mol m^{-3}.). At high concentrations (96.25 mg L^{-1} = 3.9×10^{-7} mol m^{-3}), the adsorption process obeys the Freundlich isotherm, implying the formation of multilayers. Since the adsorption of Cu^{2+} onto the substrate obeys the pseudo-second-order model, the rate-determining step is deduced to be a chemisorption process. The maximum adsorption capacity of the new adsorbent towards Cu^{2+} was 8.31 mg g^{-1} but it is less than that of commercial activated carbon (maximum adsorption capacity= 46.30 mg g^{-1}) (Yogesh *et al*., 2009). However, this substrate boasts a number of advantages such as the ease of access to starting materials, high yield of the adsorbent (96%), simple design, relatively cheap adsorbent (a rough calculation of the cost of preparation indicates 2 rupees for each gram) and easy operation. Owing to the high removal percentage, it serves as a promising substrate for the removal of Cu^{2+} from industrial effluents.

ACKNOWLEDGEMENT

The authors convey their sincere gratitude to the University of Peradeniya, Sri Lanka for providing the financial assistance for this project and to Ms. R.V.A.V.A. Wijeratne, Department of Chemistry, and the University of Peradeniya for proofreading the manuscript.

DECLARATION OF CONFLICT OF INTEREST

The authors declare no conflict of interest.

REFERENCES

Achife, E.C. and Ibemesi, J.A. (1989). Applicability of the Freundlich and Langmuir adsorption isotherms in the bleaching of rubber and melon seed oils. *Journal of the American Oil Chemists' Society* **66**(2):247-252. DOI: https://doi.org/10.1007/BF02546069.

Amarasinghe, B.M.W.P.K. and Williams, R.A.(2007).Tea waste as a low cost adsorbent for the removal of copper and lead from the water. *Chemical Engineering Journal* **132**(3): 299-309. DOI: https://doi.org/10.1016/j.cej.2007.01.016.

Amarasiri, S. (2015). Caring for water. *Greater Kandy Water Supply Project, National Water Supply and Drainage Board, Pahalakondadeniya, Katugasthota, Sri Lanka.*

Banerjee, S. and Chattopadhyaya, M.C. (2017). Adsorption characteristics for the removal of a toxic dye, tartrazine from aqueous solutions by a low-cost agricultural by-product. *Arabian Journal of Chemistry* **10**(2):1629-1638. DOI: https://doi.org/10.1016/j.arabjc.2013.06.005.

Benjamin, M.M. and Leckie J.O. (1981). Multiple-site adsorption of Cd, Cu, Zn and Pb on amorphous ironoxyhydroxide. *Colloid and Interface Science* **79**(1):209-221. DOI: https://doi.org/10.1016/00219797(81)90063-1.

Chand, R., Narimura, K., Kawakita, H. and Inoue, K.(2009). Grape waste as a biosorbent for removing Chromium (VI) from aqueous solution. *Journal of Hazardous Materials* **163**(1):245-250. DOI: https://doi.org/10.1016/j.jhazmat.2008.06.084.

Dongxiao, O., Yuting, Z., Liang, H.,Qiang, Z., Yuehua, H. and Zhiguo, H. (2019). Research on the adsorption behavior of heavy metal ions by porous material prepared with silicate tailings. *Journal of Minerals* **2019**(9):291. DOI: https://doi.org/:10.3390/min9050291.

Etim, U.J., Umoren, S.A.and Eduok, U.M. (2000). Coconut coir dust as a low-cost adsorbent for the removal of cationic dye from aqueous solution. *Journal of Saudi Chemical Society* **20**(1):67-76. DOI: https://doi.org/10.1016/j.jscs.2012.09.014

Hakan, D. and Cihan, G. (2016). Adsorption of $Cu^{2+}$from aqueous solution on activated carbon prepared from grape bagasse. *Journal of Cleaner Production***124**:103-113. DOI: https://doi.org/10.1016/j.jclepro.2016.02.084.

Jonathan, D.C., Susan, E.D. and Andrea, M.D. (2006). Evaluation of copper speciation and water quality factors that affect aqueous copper tasting response. *Chemical Senses* **31**(7):689-697. DOI: https://doi.org/10.1093/chemse/bjl010.

Kousmulski, M. (2006). pH dependent surface charging and point zero charge. *Journal of Colloid and InterfaceScience* **298**(2):730-41. DOI: https://doi.org/10.1016/j.jcis.2006.01.003 .

Langmuir, I. (1918). The adsorption of gases on plane surfaces of glass, mica and platinum. *Journal of American Chemical Society* **40**(9):1361-1403. DOI: https://doi.org/10.1021/ja02242a004.

Malkhede. S.S and Rao. Y.R.M. (2021). Sorption of Cu^{2+} ion by Adsorption using orange peel. *Journal of Physics* **1913**(1):012090. DOI: https://doi.org/10.1088/1742-6596/1913/1/012090.

Mane, V.S., Deo Mall, I. and Chandra. V. (2007). Kinetic and equilibrium isotherm studies for the adsorptive removal of Brilliant Green dye from aqueous solution by rice husk ash. *Journal of Environmental Management* **84**(4):390-400. DOI: https://doi.org/10.1016/j.jenvman.2006.06.024.

Manoj B. and Kunjomana A.G. (2012). Study of stacking structure of amorphous carbon by X-Ray diffraction technique. *International Journal of Electrochemical Science*, 7 (2012) 3127 – 3134.

Muirhead, S.J. and Furness, R.W. (1988). Heavy metal concentrations in the tissues of sea birds from,gouch island, south athlantic ocean. *Marine Pollution Bulletin* **19**(6): 278-283 DOI: .https://doi.org/10.1016/0025-326X(88)90599-1.

Nandi, B.K., Goswami, A., Das, A.K., Mondal, B. and Purkait, M.K. (2008). Kinetic and equilibrium studies on the adsorption of crystal violet dye using kaolin as an adsorbent. *Separation Science Technology* **43**(6):1382-1403. DOI: https://doi.org/10.1080/01496390701885331.

Ömer, F.K., Fahanwi, A.N. and Ufuk, Y. (2016). A response surface modelling study for sorption of

Cu^{2+}, Ni^{2+}, Zn^{2+} and Cd^{2+} using chemically modified poly(vinylpyrrolidone) and poly(vinylpyrrolidone-*co*-methylacrylate) hydrogels. *Adsorption Science and Technology***35** (4):263-283. DOI: https://doi.org/10.1177/0263617416674950.

Pehlivan, E., Yanik, B.H., Ahmetli, G.andPehlivan, M. (2008).Equilibrium isotherm studies for the uptake of cadmium and lead ions onto sugar beet pulp. *Bioresource Technology* **99**(9): 3520-3527. DOI: https://doi.org/10.1016/j.biortech.2007.07.052.

Pollard, S.J.T., Fowler, G.D., Sollars, C.J. and Perry,R. (1992). Low-cost adsorbents for waste and wastewater treatment. A review. *Science of the Total Environment* **116**(1): 31-52. DOI: https://doi.org/10.1016/0048-9697(92)90363-W.

Rais, A., Rajeev, K. and Shaziya, H. (2012). Adsorption of Cu^{2+} from aqueous solution on to iron oxide coated eggshell powder: evaluation of equilibrium, isotherms, kinetics, and regeneration capacity. *Science Direct* **5**(3): 353-359. DOI: https://doi.org/10.1016/j.arabjc.2010.09.003.

Shakila, H.P.T., Kavitha, H.R. andBupani, A.P. (2020). Adsorption Study of Cu^{2+} Ions from Aqueous solution by Bael Flowers (Aegle Marmelos). *Bio Interface Research in Applied Chemistry* **11**(4):11891-11904. DOI: https://doi.org/10.33263/ BRIAC114.1189111904.

Simonin, J.P. (2016). On the comparison of pseudo first order and pseudo second order rate laws in the modeling of adsorption kinetics. *Chemical Engineering Journal* **300**:254-266. DOI: http://dx.doi.org/10.1016/j.cej.2016.04.079.

Taimur, K., Shamsul, R.M.K. and Malay, C.(2010). Adsorptive Removal of Reactive Yellow 15 from Aqueous Solution by Coconut Coir Activated Carbon. *Adsorption science and technology* **28**(7):657-667. DOI: https://doi.org/10.1260/0263-6174.28.7.657

Volzone, C. and Garrido, L.B. (2008). Uptake of acid black 210 dye by organo montmorillonite clay materials. *Journal of Environmental Science* **88**(4):1640-1648. DOI: https://doi.org/10.5155/eurjchem.4.4.366-369.862.

Wan Ngah, W., Kamari, A. and Koay, T. (2004). Equilibrium and kinetics studies of adsorption of copper on chitosan and chitosan/PVA beads. *International Journal of Biological Macromolecules* **34**(3):155-161. DOI: https://doi.org/10.1016/j.ijbiomac.2004.03.001.

Yogesh, C.S., Uma and Siddh, N.U. (2009). Removal of a Cationic Dye from Wastewaters by Adsorption on Activated Carbon Developed from Coconut Coir. *ACS Energy and fuels* **23**(6):2983-2988. DOI: https://doi.org/10.1021/ef9001132.

Yu, B., Zhang, Y., Shukla, A. and Shukla, S.S. (2001). The removal of heavy metals from aqueous solution by saw dust adsorption – removal of lead and comparison of its adsorption with copper. *Journal of Hazardous Materials* **84**(1):83-94. DOI: https://doi.org/:10.1016/s0304-3894(01)00198-4.